

Articles

Discovery and Pharmacological Evaluation of Growth Hormone Secretagogue Receptor Antagonists

Zhili Xin,* Michael D. Serby, Hongyu Zhao, Christi Kosogof, Bruce G. Szczepankiewicz, Mei Liu, BoLiu, Charles W. Hutchins, Kathy A. Sarris, Ethan D. Hoff, H. Douglas Falls, Chun W. Lin, Christopher A. Ogiela, Christine A. Collins, Michael E. Brune, Eugene N. Bush, Brian A. Droz, Thomas A. Fey, Victoria E. Knourek-Segel, Robin Shapiro, Peer B. Jacobson, David W. A. Beno, Teresa M. Turner, Hing L. Sham, and Gang Liu

Metabolic Disease Research, Global Pharmaceutical Research and Development, Abbott Laboratories, 100 Abbott Park Road, Abbott Park, Illinois 60064-6098.

Received April 18, 2006

The discovery and pharmacological evaluation of potent, selective, and orally bioavailable growth hormone secretagogue receptor (GHS-R) antagonists are reported. Previously, 2,4-diaminopyrimidine-based GHS-R antagonists reported from our laboratories have been shown to be dihydrofolate reductase (DHFR) inhibitors. By comparing the X-ray crystal structure of DHFR docked with our GHS-R antagonists and GHS-R modeling, we designed and synthesized a series of potent and DHFR selective GHS-R antagonists with good pharmacokinetic (PK) profiles. An amide derivative **13d** (Ca^{2+} flux IC_{50} = 188 nM, [brain]/[plasma] = 0.97 @ 8 h in rat) showed a 10% decrease in 24 h food intake in rats, and over 5% body weight reduction after 14-day oral treatment in diet-induced obese (DIO) mice. In comparison, a urea derivative **14c** (Ca^{2+} flux IC_{50} = 7 nM, [brain]/[plasma] = 0.0 in DIO) failed to show significant effect on food intake in the acute feeding DIO model. These observations demonstrated for the first time that peripheral GHS-R blockage with small molecule GHS-R antagonists might not be sufficient for suppressing appetite and inducing body weight reduction.

Introduction

The growth hormone secretagogue receptor (GHS-R^a), a recently de-orphaned G-protein coupled receptor (GPCR), has attracted tremendous attention in the past decade.¹ GHS-R is structurally distinct from the growth hormone releasing hormone (GHR-H) receptor, the principal regulator of growth hormone release, and constitutes an alternative physiological system for the regulation of growth hormone secretion. The GHS-R is expressed widely in the brain and peripheral tissues, especially in stomach and intestine. In 1999, Kojima and co-workers successfully isolated and identified the endogenous ligand for the GHS-R from rat stomach and named it “ghrelin”.² Ghrelin, a 28 amino acid peptide in which serine-3 (Ser3) is uniquely *n*-octanoylated, is secreted predominantly from the stomach and small intestine, although it is also produced in the kidneys, pancreas, and hypothalamus.³ Ghrelin exhibits a wide range of biological activities.^{4,5} It not only elevates plasma levels of growth hormone, but also increases food intake. In rodents, ghrelin plasma levels increase sharply on fasting.⁶ In humans, ghrelin levels rise prior to each meal and decrease after eating.⁷ Furthermore, intravenous (i.v.) administration of ghrelin to humans causes hunger and results in increased food consumption. In addition to acute effects on food intake, ghrelin also affects body weight and adiposity. Chronic administration of

ghrelin in freely feeding mice and rats results in increased body weight and decreased fat utilization.⁸

Since ghrelin appears to play an important role in meal-initiation and regulation of energy balance, GHS-R (ghrelin receptor) antagonists are expected to reduce food intake and body weight and therefore provide a potentially novel treatment for obesity. Unfortunately, there have been very few literature reports on the pharmacological intervention of ghrelin action in adult animal models. It has been shown that a single intracerebroventricular administration of anti-ghrelin IgG reduced daily food intake and body weight in lean rats.⁸ Further evidence of GHS-R antagonism induced metabolic effects came from peripheral administration of [D-Lys-3]-GHRP-6, a peptide GHS-R antagonist, resulted in reduction of food intake and body weight gain in mice.⁹ More recently, NOX-B11-2, a ghrelin-neutralizing RNA Spiegelmer (SPM), was shown to evoke body weight loss in DIO mice with reduced food intake and fat mass relative to control SPM-infused mice.¹⁰

Among the few GHS-R antagonists reported in the literature, compound **1**¹¹ (L-692400, Figure 1) is the first nonpeptidyl antagonist, but no activity against GHS-R or structure activity relationship (SAR) was reported. Since 2003, several groups have disclosed small molecule GHS-R antagonists in the patent literature with limited biological data.¹² We have previously reported our investigations into the isoxazole and tetralin carboxamide classes of GHS-R antagonists (**2** and **3**, Figure 1).^{13–16} The poor bioavailabilities of isoxazole carboxamides **2** prevented their further development. Tetralin derivative **3a** (Ca^{2+} flux IC_{50} = 33 nM) possessed moderate oral bioavailability (F = 21%) and low brain permeability, with a brain-to-plasma ratio of 0.12 at 1 h after intravenous dosing in rats. However, there

* To whom correspondence should be addressed. Tel: 847-935-7307. Fax: 847-938-1674. E-mail: zhili.xin@abbott.com.

^a Abbreviations: GHS-R, growth hormone secretagogue receptor; DHFR, dihydrofolate reductase; SPM, Spiegelmer; DIO, diet-induced obese; DEXA, dual energy X-ray absorptiometry; NPY, neuropeptide Y; Agrp, agouti-related protein; RME, relative mass error.

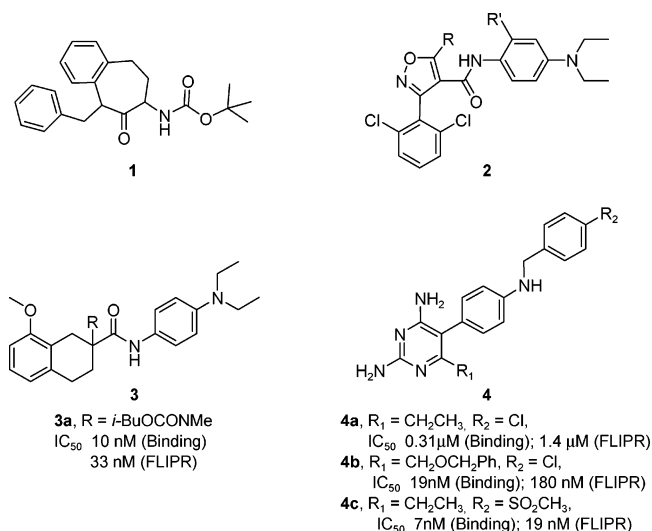


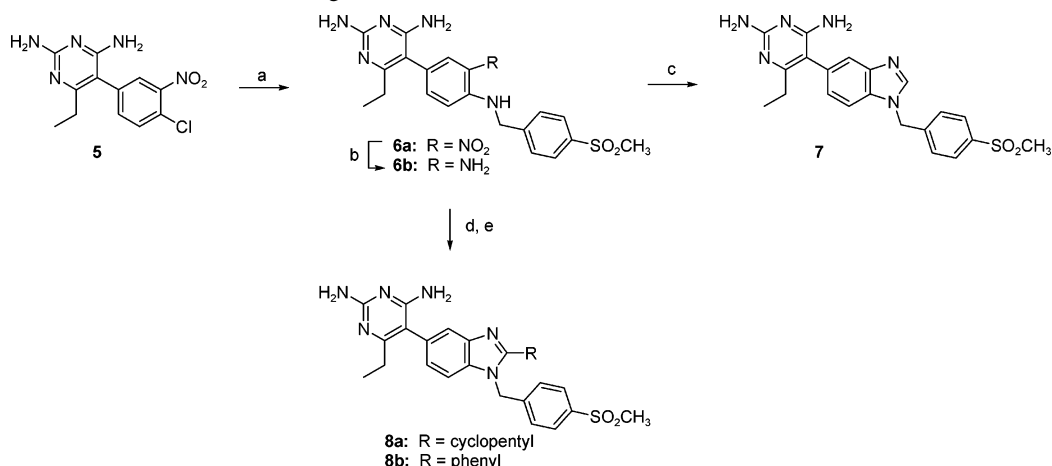
Figure 1. Small molecule GHS-R antagonists.

was no significant effect of **3a** on feeding and body weight in free-fed or fasted rats due to insufficient drug exposure in both plasma and brain (unpublished results).

A series of GHS-R antagonists featuring a 2,4-diaminopyrimidine pharmacophore was identified from a high throughput screen (HTS). Hit compound **4a** (Figure 1), with an IC₅₀ of 0.3 μM in a radioligand binding assay and 1.4 μM in a cell-based Ca²⁺ flux functional assay, showed a desirable pharmacokinetic profile with greater than 75% oral bioavailability. SAR exploration led to both binding and functional potency improvements through extension of the ethyl side chain and modification of the *p*-chlorobenzyl group, as shown by **4b** and **4c** (Figure 1). Compound **4b** (binding IC₅₀ = 19 nM; Ca²⁺ flux IC₅₀ = 180 nM) was the first small molecule GHS-R antagonist to demonstrate *in vivo* efficacy in our laboratories.¹⁷ Intraperitoneal (i.p.) administration of **4b** caused a decrease in food intake in overnight fasted or free-fed rats and attenuated body weight regain following caloric restriction in diet-induced obese (DIO) mice.

Compound **4b** efficiently partitioned into the brain, with a brain-to-plasma ratio of 3.1 and 1.4 at 1 and 8 h respectively after intravenous dosing in rats. The oral bioavailability (*F* = 5.5%) of **4b** was, however, insufficient for oral dosing. Compound **4c**, with an ethyl side chain, was discovered as more potent (binding IC₅₀ = 7 nM; Ca²⁺ flux IC₅₀ = 19 nM) GHS-R antagonist with desirable oral bioavailability (*F* = 52%, rat).

Scheme 1. Synthesis of Benzoimidazole Analogues^a



^a Reagents: (a) 4-Methylsulfonylbenzylamine hydrochloride, Hunig's base, NMP, microwave 190 °C, 40 min; (b) SnCl₂·2H₂O, EtOH, reflux, 1 h; (c) HCOOH, 110 °C, 1 h (d) Carbonyl chloride, THF; (e) Polyphosphoric acid, 150 °C.

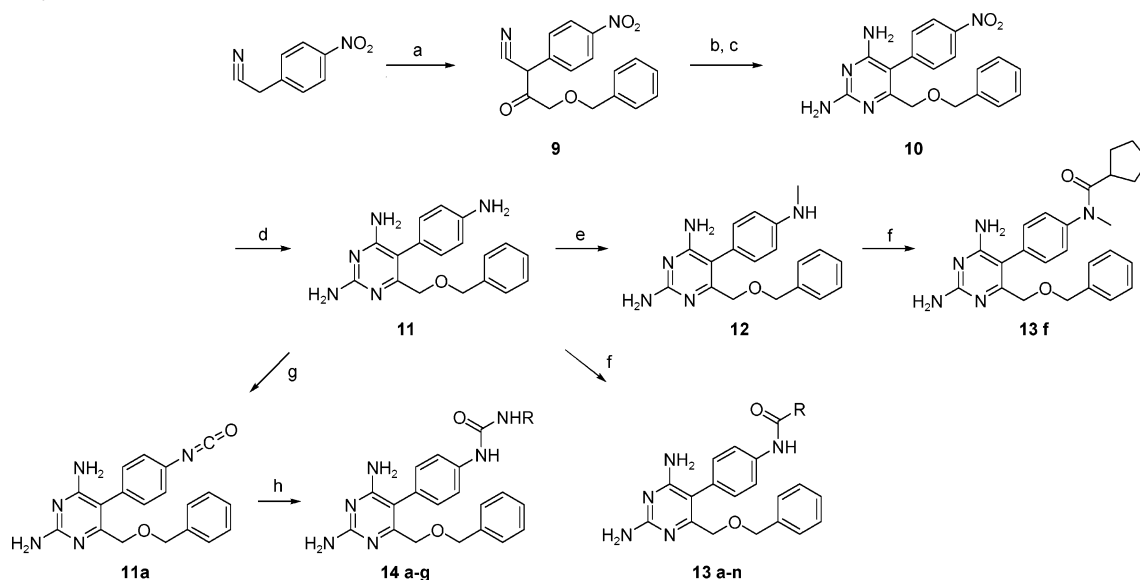
Diaminopyrimidine derivative **4c** was evaluated in acute and subchronic rodent feeding models. To our disappointment, signs of stress (diarrhea) were observed in DIO mice. 2,4-diaminopyrimidine is a well-known privileged pharmacophore for DHFR inhibitors, such as trimetrexate and pyrimethamine,¹⁸ and trimetrexate is known to cause severe bloody diarrhea at 6 mg/kg doses in normal dogs.¹⁹ Our 2,4-diaminopyrimidine-based GHS-R antagonists with general structure of **4** were found to inhibit human DHFR effectively (IC₅₀ < 1 μM) in most cases. Compound **4c**, in particular, exhibited an IC₅₀ value less than 10 nM versus hDHFR. While we believed that *in vivo* efficacy observed with compound **4b** (hDHFR IC₅₀ ~ 0.3 μM) was at least in part due to antagonism of GHS-R,¹⁷ achieving adequate selectivity (> 1000-fold) over DHFR became a major focus of our GHS-R antagonist program. We docked our GHS-R antagonist **4c** with available DHFR crystal structures and compared its binding modes with those for GHS-R and identified regions of the molecule for possible divergence of structure–activity relationships (SAR). In this paper, we present our discovery of diaminopyrimidine-based amide and urea derivatives as potent, DHFR selective and orally bioavailable GHS-R antagonists and describe the pharmacological evaluation of two select analogues (**13d** and **14c**) in obesity rodent models.

Chemistry. The synthetic procedures employed for the preparation of diaminopyrimidines bearing benzimidazole substituents are outlined in Scheme 1. Diaminopyrimidine **5**²⁰ was used as a key starting material for the syntheses of target compounds. After displacement of the chloride with 4-(methylsulfonyl)benzylamine,²¹ the nitro group was reduced with tin(II) chloride to provide aniline **6b**,²⁰ which was heated with HCOOH to give benzimidazole **7**.²² For the 2-substituted benzimidazole analogues **8a** and **8b**, acid chlorides were used to acylate intermediate **6b**,²³ followed by cyclization with polyphosphoric acid.

To generate various amides and ureas, aniline **11** was prepared according to our previously described procedure and used as a key building block (Scheme 2).¹⁷ Acylation of **11** with various carboxylic acids using TBTU as a coupling reagent was straightforward, giving amides **13a–n**. To make urea derivatives, we prepared isocyanate **11a** from aniline **11** using triphosgene.²⁴ Treatment of **11a** *in situ* with various amines proceeded smoothly to provide urea **14a–g**.

Results and Discussion

With potent GHS-R antagonists, e.g. **4c**, in hand, we sought to diminish the DHFR inhibitory activity exhibited by these

Scheme 2. Synthesis of Ureas and Amides^a

^a Reagents: (a) Benzyloxyacetyl chloride, TEA, DMAP, CH_2Cl_2 ; (b) TMSCHN_2 , Et_2O ; (c) guanidine, EtOH , reflux; (d) $\text{Pd}(\text{OH})_2/\text{C}$, H_2 (60 psi), MeOH ; (e) HCHO , NaBH_3CN , AcOH , MeOH ; (f) Acids, TBTU, Hunig's base, DMF ; (g) triphosgene, Hunig's base, THF , r.t.; (h) amines, r.t.

analogues. At first, our chemistry effort was focused on modifying the 2,4-diaminopyrimidine core structure, since it is also the required pharmacophore for DHFR inhibition. Unfortunately, all attempts to replace the pyrimidine core with pyridine or other heterocyclic rings resulted in the complete disappearance of GHS-R antagonist activity. Removal or replacement of any NH_2 group on the pyrimidine ring also reduced activity dramatically. However, extension of the pyrimidine 6-alkyl side chain was tolerated.^{17,25} As a matter of fact, significant improvement of the GHS-R inhibitory potency and some DHFR selectivity was realized by introducing different ether or amine moieties at the 6-pyrimidine position. However, more significant improvement in DHFR selectivity was still needed to enable effective and interpretable *in vivo* pharmacology studies.

Since we did not achieve our desired DHFR selectivity via 2,4-diaminopyrimidine core modifications, we turned our attention to the periphery of the molecule. The X-ray crystal structures of diaminopyrimidines in complex with mammalian DHFR have been known since 1989.²⁶ Using these crystal structures as a template, we anchored the diaminopyrimidine of **4c** and docked the rest of the molecule into DHFR, as shown in Figure 2b. In the meantime, we also modeled some potential binding modes of **4c** with GHS-R using a proprietary GPCR model, which was developed based on the dopamine receptor model.^{27–29} One of the low energy binding modes is shown in Figure 2a. Comparing the binding modes represented by Figures 2a and 2b, we noticed that there was additional space between the GHS-R surface and the pyrimidine 5-aryl or distal benzylamine groups of **4c**, whereas **4c** binding to DHFR offered less room about these regions. We hypothesized that elaborating this region of the inhibitor could allow us to pick up additional binding affinity with GHS-R, while disrupting DHFR binding at the same time. Benzimidazole analogues **7** and **8** represent manifestations of this hypothesis. The imidazole fused to the 5-aryl ring offered slightly improved binding affinity for GHS-R (4 nM for **7** vs 7 nM for **4c**). On the other hand, DHFR inhibitory activity of **7** was diminished (78% inhibition @ 1 μM) compared to **4c** ($\text{IC}_{50} < 10 \text{ nM}$; 99% inhibition @ 1 μM). To further improve DHFR selectivity, we introduced cyclic substituents into 2-position of the imidazole (**8a**, **8b**). It was not surprising to see that IC_{50} values for DHFR were further

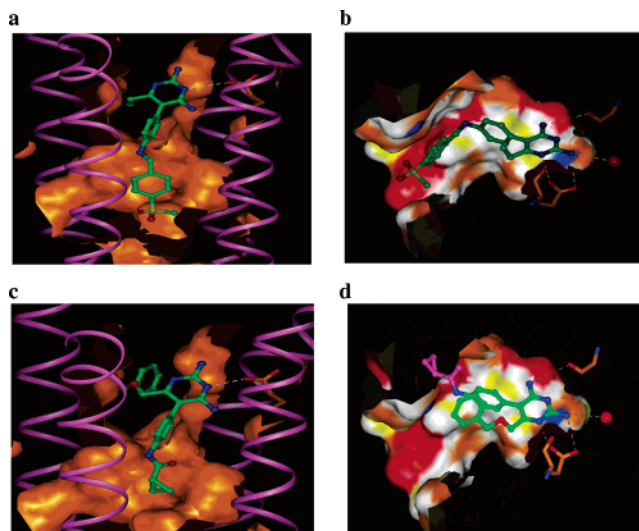


Figure 2. Molecular model of antagonists docked in the binding pocket of GHS-R and DHFR. (a) **4c** in receptor. (b) **4c** in DHFR. (c) **13d** in receptor. (d) **13d** in DHFR.

increased to the micromolar range. However, 2-imidazole substituents were also detrimental to GHS-R binding affinity. Nevertheless, both **8a** and **8b** exhibited over 100-fold selectivity over DHFR.

An alternative approach to achieve DHFR selectivity was restricting the flexibility of benzylamine group. It was suggested by the molecular modeling that an amide group in the place of the aminomethyl group would be acceptable in GHS-R (**13d** in Figure 2c), whereas it would protrude through the DHFR surface (**13d** in Figure 2d). The first encouraging result emerged from amide analogue **13d**. It has Ca^{2+} flux IC_{50} of 188 nM, similar to our lead compound **4b** (180 nM), while it showed markedly reduced DHFR inhibitory activity ($\text{IC}_{50} = 28 \mu\text{M}$), compared to 0.3 μM of **4b**. Compound **13d** exhibited a good pharmacokinetic profile in rats ($F = 32\%$, $t_{1/2} = 2.4 \text{ h}$, oral $\text{AUC} = 0.82 \mu\text{g}\cdot\text{h/mL}$). More importantly, reasonable brain penetration of **13d** was detected with brain/plasma ratios of 0.26 (1 h), 1.1 (4 h), and 0.97 (8 h) at various post-dosing time-points. These results prompted further examination and optimization of the

Table 1. Diaminopyrimidine Key SAR with Central Core Modifications

| Compound # | Structure | Binding IC ₅₀ ± SEM (nM) ^a | Ca ²⁺ flux IC ₅₀ ± SEM (nM) ^a | hDHFR IC ₅₀ |
|------------|-----------|--|--|------------------------|
| 4c | | 7 ± 2 | 19 ± 12 | <10 nM 99% @ 1μM |
| 7 | | 4 ± 2 | 11 ± 8 | 78% @ 1μM |
| 8a | | 8 ± 2 | 109 ± 22 | 1.83μM |
| 8b | | 16 ± 1 | 249 ± 61 | 2.3μM |

^a Results are given as the mean of more than or equal to two independent experiments if not specified.

amide region. Table 2 outlines the key SAR of this region. In general, hydrophobic carboxylic acids yielded amides with the best GHS-R antagonist activity. This is probably due to a favorable lipophilic interaction with GHS-R. Consistent with this hypothesis, more polar groups, such as pyridines in **13h** and **13i**, generated less potent antagonists. The amide N–H appeared to be important, as tertiary amide **13f** was about 100-fold less potent than secondary amide **13e**. High selectivity against DHFR was observed with every amide we tested, with IC₅₀ values greater than 10 μM in hDHFR assay (**13d–m** in Table 4). In the case of **13e**, >250-fold selectivity was achieved.

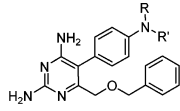
Encouraged by the promising results with amide derivatives, we next investigated urea analogues, which are structurally more rigid and less prone to be cleaved by amidases. It was gratifying to find that most urea analogues had very potent GHS-R activity, while DHFR activity was insignificant (**14a–g** in Table 4). The SAR trend was similar to that was observed with the amide series (Table 3). In most cases, ureas showed superior antagonist activity to their amide analogues (**14a** vs **13c**, **14e** vs **13n**). N,N-Disubstitution of the urea was detrimental to activity as **14b** (R = Me, Ca²⁺ flux IC₅₀ >10 μM) was considerably less potent than analogue **14a** (R = H, Ca²⁺ flux IC₅₀ = 56 nM). Compound **14c** exhibited low nanomolar activity in Ca²⁺ flux assays, as well as exquisite selectivity over DHFR (IC₅₀ > 100 μM). More importantly, urea **14c** also exhibited favorable pharmacokinetic properties in DIO mice after oral dosing (*t*_{1/2} = 4.5 h; oral AUC = 12.3 μg.h/mL). However, no compound **14c** could be detected in the brain tissue of DIO mice following oral dosing.

With potent, DHFR selective, oral bioavailable GHS-R antagonists (i.e. **13d** and **14c**) in hands, we turned our attention to evaluating the effectiveness of analogues **13d** and **14c** in suppressing feeding and inducing body weight reduction in rodents. For GHS-R antagonist **13d** tested in the acute feeding model, we administered two doses of the compound before the beginning of the dark phase of the light cycle to maximize the suppression of orexigenic signal induced by ghrelin. So, in this model, **13d** was dosed orally twice to Sprague–Dawley rats at

15 and 50 mg/kg within 8 h interval. A significant (9–11%) decrease in cumulative food intake after 24 to 32 h post last dose was observed for the 50 mg/kg dosing group (Figure 3). When dosed at 50 mg/kg, **13d** maintained plasma exposure levels 6 to 61-fold above the in vitro binding IC₅₀ (66 nM) for up to 24 h, and the brain levels were about 2–9-fold above that concentration.

Encouraged by the positive signal in the acute model, we also evaluated **13d** for its effects on food intake and body weight upon subchronic treatment (p.o.) in DIO mice (Figure 4). Compound **13d** and vehicle were dosed twice daily for 2 weeks in a standard protocol in 25-week-old male C57BL/6J mice with high fat diet-induced obesity. Oral administration of **13d** at 50 mg/kg doses resulted in a significant decrease in food intake on the first day, although cumulative food intake was the same for both groups after 4 days (Figure 4a). About 2 g (5.4%) body weight reduction was observed at the end of the 14-day study (Figure 4b), accompanied by a significant decrease (~20%) in epididymal fat pad weight (Figure 5a) with no change in lean body mass as measured by dual energy X-ray absorptiometry (DEXA) scanning. Plasma insulin levels were significantly reduced with treatment (Figure 5b), but leptin levels were not statistically different. There was no change in the liver enzymes (ALT, AST) activities for compound **13d** treatment group as compared to vehicle treated group (data not shown).

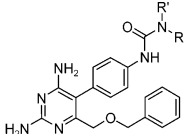
Since urea **14c** exhibited favorable pharmacokinetic properties in DIO mice, we evaluated its effects on acute food intake in a protocol analogous to that used by Asakawa et al, who demonstrated that the peptide antagonist [D-Lys-3]-GHRP-6 decreased food intake in fasted lean mice.⁹ Our study would compare the effects of our diaminopyrimidine-based urea **14c** (dosed orally) to benzylamine analogue **4b** along with [D-Lys-3]-GHRP-6 which were administered (i.p.) to fasted DIO mice. The results are summarized in Figure 6 with the Y-axis expressing food intake data as percent of vehicle control to better visualize the magnitude of decreased food intake. The 5 mg/kg dose of [D-Lys-3]-GHRP-6 in our study equaled to the 200 nmol/mouse dose used by Asakawa et al. As shown in Figure 6, the

Table 2. Key SAR of Selected Amide Derivatives of Diaminopyrimidine


| Compound # | R | R' | Binding IC ₅₀ ± SEM (nM) | Ca ²⁺ flux IC ₅₀ ± SEM (nM) |
|------------|-----------------|----|-------------------------------------|---|
| 13a | H | | 2270 | >10000 |
| 13b | H | | 221 ± 30 | >10000 |
| 13c | H | | 72 ± 24 | 108 |
| 13d | H | | 66 ± 23 | 188 ± 30 |
| 13e | H | | 18 ± 13 | 40 ± 28 |
| 13f | CH ₃ | | 1670 | >10000 |
| 13g | H | | 391 ± 170 | >10000 |
| 13h | H | | 3080 | >10000 |
| 13i | H | | >1000 | >10000 |
| 13j | H | | 126 | >10000 |
| 13k | H | | 70 | 382 ± 140 |
| 13l | H | | 41 ± 29 | 137 ± 64 |
| 13m | H | | 37 ± 15 | 408 ± 280 |
| 13n | H | | 47 ± 14 | 343 ± 130 |

peptide antagonist [D-Lys-3]-GHRP-6 reduced cumulative food intake by about 65% at 20 min, consistent with a published report. GHS-R antagonist **4b** (dosed @ 30 mg/kg) decreased food intake more than 86% at 20 min, consistent with earlier reported data in a rat model.¹⁷ However, the effect caused by **14c** (dosed @ 100 mg/kg) was not statistically significant although the mean inhibition was 40–60% at 20 min and 1 h time points. A small and variable feeding signal at those early time points contributes to the lack of significance. Lower dose of **14c** @ 30 mg/kg showed similar degree of food intake inhibition and signal variability. Only antagonist **4b** showed significant effect in food intake suppression at later time points (2 h, 4 h, and 24 h), while neither peptide nor **14c** showed significant suppression of accumulative food intake at those time points.

The exact pathways by which ghrelin regulates food intake in vivo have remained controversial.³⁰ Genetic experiments along with earlier pharmacologic data demonstrated that the combination of neuropeptide Y (NPY) and agouti-related protein (Agrp) is required for ghrelin-induced feeding. One model has suggested that ghrelin is a neurocrine peptide that stimulates food intake through its receptor expressed on afferent vagal

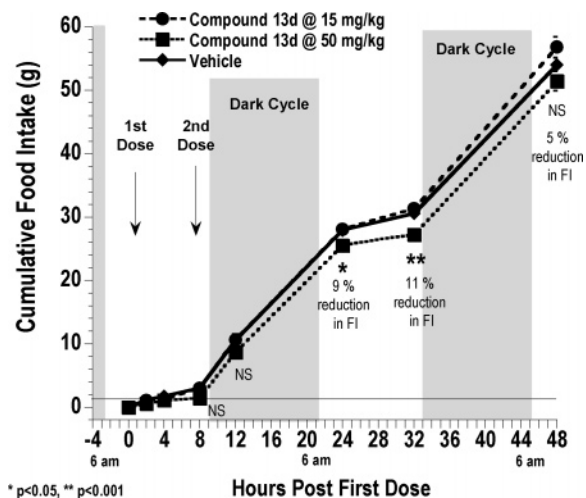
Table 3. Key SAR of Selected Urea Derivatives of Diaminopyrimidine


| Compound # | R | R' | Ca ²⁺ flux IC ₅₀ ± SEM (nM) |
|------------|----|----|---|
| 14a | H | | 56 ± 22 |
| 14b | Me | | > 10000 |
| 14c | H | | 7 ± 1 |
| 14d | H | | 88 |
| 14e | H | | 34 ± 6 |
| 14f | H | | 10 ± 3 |
| 14g | H | | 7 ± 4 |

Table 4. DHFR Selectivity of Representative Amide and Urea Derivatives of Diaminopyrimidine

| Compound # | Ca ²⁺ flux IC ₅₀ (μM) | DHFR IC ₅₀ (μM) ^a |
|------------|---|---|
| 13d | 0.188 | 28 |
| 13e | 0.040 | > 10 |
| 13l | 0.137 | > 10 |
| 13m | 0.408 | > 10 |
| 14a | 0.056 | > 10 |
| 14c | 0.007 | > 100 |
| 14d | 0.088 | > 10 |
| 14g | 0.007 | > 10 |

^a IC₅₀ of hDHFR was reported as > 10 μM for the compound with < 50% inhibition @ 10 μM and poor solubility to test on higher concentration.

**Figure 3.** Acute study of GHS-R antagonist on food intake in rats: compound **13d** reduced cumulative food intake at 24 and 32 h.

nerve terminals in the foregut, thereby signaling to the hindbrain and indirectly to the hypothalamus.³¹ It has been well-established that rodents with vagotomy are not sensitive to the feeding effects of ghrelin.^{31,32} More recently, similar observation has been made in patients who had a previous complete truncal vagotomy with lower esophageal or gastric surgery experienced

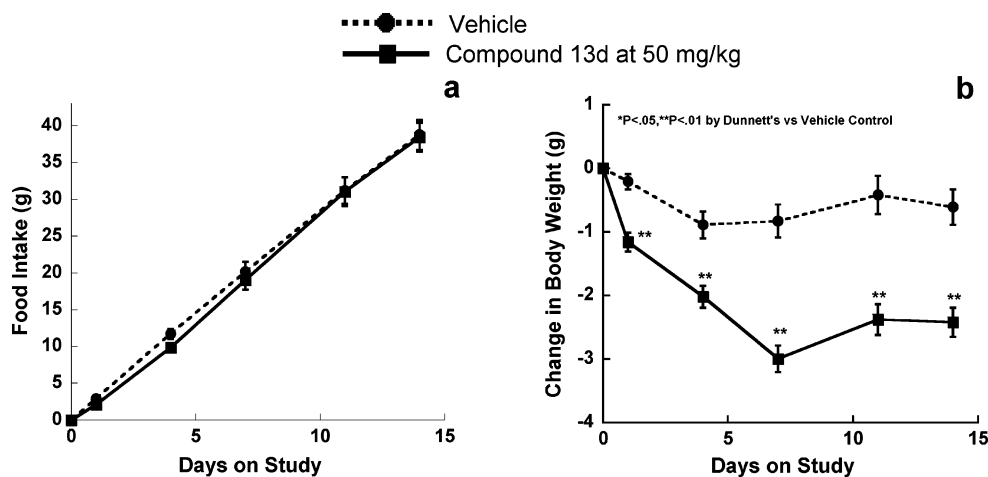


Figure 4. Effects of subchronic (14 days) treatment (p.o.) of GHSR antagonist **13d** on body weight and food intake in male C57BL/6J mice with diet-induced obesity.

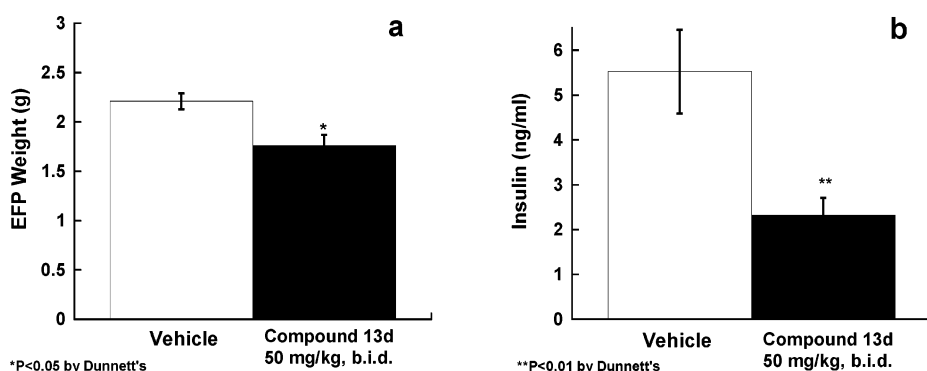


Figure 5. Effects of 14 days treatment with compound **13d** on fat mass and insulin levels in DIO mice.

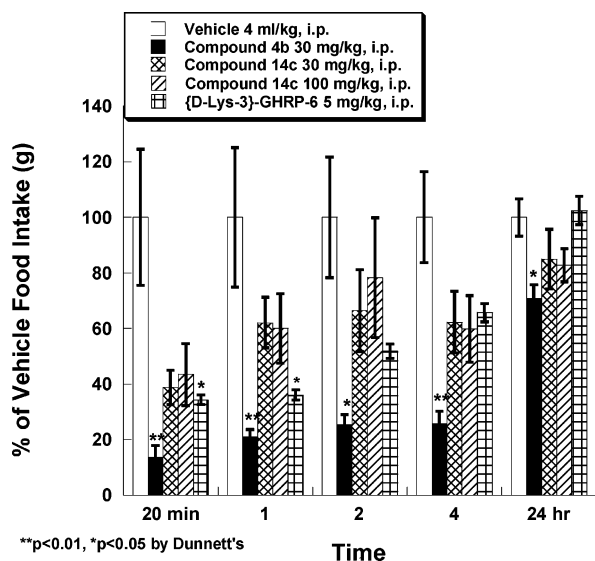


Figure 6. Effects of acute administration (i.p.) of antagonists on food intake in fasted DIO mice.

no food intake change upon ghrelin infusion (1 pmol/kg·min ghrelin, and 5 pmol/kg·min ghrelin, respectively).³³ These results seemed to suggest that peripheral blockade of ghrelin receptors with small molecule antagonists could act as chemical vagotomy and block the effects of ghrelin actions. It is obvious that compared to **4b**, urea analogue **14c** had much less effect on food intake in this model. The fact that **14c** has improved in vitro potency and PK profile with essentially no brain penetration suggested peripheral ghrelin blockage might not be suf-

ficient for achieving the anticipated efficacy in appetite suppression and body weight regulation via ghrelin antagonism. For antiobesity indication with GHS-R antagonists, central inhibition of the activity of GHS-Rs on the NPY/AgRP-expressing neurons in the hypothalamus and neurons in the circumventricular sites in the hindbrain are probably required.

Conclusion

Potent, DHFR-selective, and orally bioavailable diaminopyrimidine-based GHS-R antagonists were identified. The molecular modeling studies using the published DHFR X-ray structure and in-house GHS-R model provided structural insights for imparting DHFR selectivity to diaminopyrimidine-based GHS-R antagonists. Introduction of an amide or urea moiety to the molecule restrained the flexibility of the original benzylamine linker and provided remarkable selectivity against DHFR. An amide derivative **13d** showed a 10% decrease in 24 h food intake in rats and over 5% body weight reduction after 14-day oral treatment in DIO mice. The in vivo results from **14c** and **4b** on the acute DIO model studies suggested that the penetration of blood–brain barrier is probably necessary for an antagonist to block ghrelin's orexigenic effects. Even though GHS-R antagonist **14c** did not provide the desirable phenotypes in metabolic disease models, it may still be a valuable tool compound for elucidating the other potential therapeutic benefits for a periphery-acting GHS-R antagonist.¹

Experimental Section

General Information. Unless otherwise specified, all solvents and reagents were obtained from commercial suppliers and used without further purification. Flash chromatography was performed

using silica gel (230–400 mesh) from E. M. Science. ^1H NMR spectra were recorded on a Varian Mercury 300 (300 MHz), Varian UNITY 400 (400 MHz) spectrometer and are reported in ppm (δ) from tetramethylsilane (TMS: δ 0.0 ppm). Data are reported as follows: chemical shift, multiplicity (*s* = singlet, *brs* = broad singlet, *d* = doublet, *t* = triplet, *q* = quartet, *m* = multiplet, *dd* = doublet of doublet, *ddd* = doublet of doublet of doublet), coupling constants (Hz), integration. Mass spectral analyses were accomplished on a Finnigan SSQ7000 GC/MS mass spectrometer using different techniques, including electrospray ionization (ESI), and atmospheric pressure chemical ionization (APCI), as specified for individual compounds. Exact mass measurement was performed on a Finnigan FTMS Newstar T70 mass spectrometer. The compound is determined to be “consistent” with the chemical formula if the exact mass measurement is within 5.0 ppm relative mass error (RME) of the exact monoisotopic mass.

Analytical HPLC for selected compounds were performed on two systems: System A: Samples were analyzed by a Gilson analytical HPLC system, using an YMC C-8 column (50 \times 4.6 mm i.d., S-5 μm , 120 \AA). The solvent system used was acetonitrile/0.1% aqueous NH_4OAc , gradient 0–70% over 15 min @ 2 mL/min. System B: Samples were analyzed by Agilent Analytical HPLC 1100 Series, SB-C8 column (Zorbax 3.5 μm , 4.6 \times 75 mm). Solvent system used was acetonitrile/0.1% aqueous TFA, gradient 10–70% over 10 min @ 1.5 mL/min. The purity of the compounds was determined on two analytic HPLC systems to be of greater than 95% purity by UV detection.

Preparative reverse phase HPLC was performed on an automated Gilson HPLC system, using a SymmetryPrep Shield RP18 prep cartridge, 25 mm \times 100 mm i.d., S-7 μm , and a flow rate of 25 mL/min; λ = 214, 245 nm; mobile phase A, 0.1% TFA or NH_4OAc in H_2O ; mobile phase B, CH_3CN ; linear gradient 0–70% of B in 19 min. The purified fractions were evaporated to dryness on a ThermoSavant SpeedVac.

5-[3-Amino-4-(4-methanesulfonyl-benzylamino)-phenyl]-6-ethyl-pyrimidine-2,4-diamine (compound 6b). This intermediate was prepared from **5** via a two-step sequence. To a solution of diaminopyrimidine **5** (176 mg, 0.6 mmol) in NMP (3.0 mL) were added 4-methanesulfonyl benzylamine hydrochloride (266 mg, 1.2 mmol) and *N,N'*-diisopropylethylamine (420 μL , 2.4 mmol). The reaction mixture was heated at 190 $^\circ\text{C}$ for 40 min in a Personal Chemistry Optimizer microwave reactor. The same reaction was repeated two more times. The combined reaction mixtures were diluted with saturated NaHCO_3 solution (50 mL) and extracted with EtOAc (100 mL). The organic layer was washed with H_2O (30 mL) and brine (3 \times 30 mL), dried over MgSO_4 , and concentrated in vacuo. The residue was triturated with acetonitrile to give intermediate **6a** as a yellow solid (150 mg, 19% yield). ^1H NMR (300 MHz, $\text{DMSO}-d_6$) δ 8.82 (t, *J* = 6.1 Hz, 1H), 7.92 (d, *J* = 8.5 Hz, 2H), 7.84 (d, *J* = 2.4 Hz, 1H), 7.68 (d, *J* = 8.5 Hz, 2H), 7.25 (dd, *J* = 2.0, 8.8 Hz, 1H), 6.93 (d, *J* = 8.8 Hz, 1H), 5.82 (s, 2H), 5.63 (s, 2H), 4.78 (d, *J* = 6.1 Hz, 2H), 3.20 (s, 3H), 2.09 (q, *J* = 7.5 Hz, 2H), 0.95 (t, *J* = 7.5 Hz, 3H). MS (ESI) *m/e* 443 ($\text{M} + \text{H}$) $^+$.

To a suspension of **6a** (145 mg, 0.33 mmol) in ethanol (7 mL) was added tin(II) chloride dihydrate (370 mg, 1.64 mmol). The reaction mixture was heated to reflux for 1 h and then cooled to room temperature and partitioned between ethyl acetate (50 mL) and saturated NaHCO_3 (50 mL). The organic phase was washed with brine (30 mL), dried over MgSO_4 , concentrated, and triturated with CH_3CN to provide aniline **6b** as a yellow solid (128 mg, 95% yield). ^1H NMR (300 MHz, $\text{DMSO}-d_6$) δ 7.90 (d, *J* = 8.5 Hz, 2H), 7.67 (d, *J* = 8.5 Hz, 2H), 6.40 (d, *J* = 2.0 Hz, 1H), 6.35 (d, *J* = 8.1 Hz, 1H), 6.24 (dd, *J* = 2.0, 8.1 Hz, 1H), 5.68 (s, 2H), 5.34 (t, *J* = 5.8 Hz, 1H), 5.21 (brs, 2H), 4.67 (s, 2H), 4.43 (d, *J* = 5.8 Hz, 2H), 3.20 (s, 3H), 2.13 (q, *J* = 7.5 Hz, 2H), 0.95 (t, *J* = 7.5 Hz, 3H). MS (ESI) *m/e* 413 ($\text{M} + \text{H}$) $^+$.

6-Ethyl-5-[1-(4-methanesulfonyl-benzyl)-1H-benzimidazol-5-yl]-pyrimidine-2,4-diamine (compound 7). The solution of aniline **6b** (83 mg, 0.2 mmol) in HCOOH (500 μL) was heated at 110 $^\circ\text{C}$ for 1 h, allowed to cool to room temperature, and partitioned

between ethyl acetate (30 mL) and saturated NaHCO_3 (20 mL). The organic phase was washed with brine (20 mL) and water (3 \times 20 mL), concentrated in vacuo, and triturated with CH_3CN to provide compound **7** as an off-white solid (81 mg, 96% yield). ^1H NMR (300 MHz, $\text{DMSO}-d_6$) δ 8.48 (s, 1H), 7.93 (d, *J* = 8.5 Hz, 2H), 7.64 (d, *J* = 8.5 Hz, 2H), 7.60 (d, *J* = 7.8 Hz, 1H), 7.44 (d, *J* = 1.4 Hz, 1H), 7.01 (dd, *J* = 1.4, 7.8 Hz, 1H), 5.78 (s, 2H), 5.65 (s, 2H), 5.36 (brs, 2H), 3.19 (s, 3H), 2.13 (q, *J* = 7.5 Hz, 2H), 0.94 (t, *J* = 7.5 Hz, 3H). HRMS (ESI) calcd for $\text{C}_{21}\text{H}_{23}\text{N}_6\text{O}_2\text{S}$ ($\text{M} + \text{H}$) $^+$ 423.1598, found 423.1598.

General Procedure for Synthesis of Benzimidazole Derivative: 5-[2-Cyclopentyl-1-(4-methanesulfonyl-benzyl)-1H-benzimidazol-5-yl]-6-ethyl-pyrimidine-2,4-diamine (compound 8a). To a solution of **6b** (50 mg, 0.113 mmol) in THF (1.1 mL) was added cyclopentanecarbonyl chloride (14 μL , 0.113 mmol). After 1 h at room temperature, the reaction mixture was concentrated in vacuo, taken up in saturated NaHCO_3 solution. The yellow solid was isolated (55 mg, 95% yield). It was dissolved in polyphosphoric acid (0.5 mL), heated to 150 $^\circ\text{C}$ for 1 h, allowed to cool to room temperature, diluted with H_2O , and basified with 50% NaOH solution to pH = 10. The solid was collected and triturated with CH_3CN . A light brown solid was isolated (20 mg, 38% yield). ^1H NMR (300 MHz, $\text{DMSO}-d_6$) δ 7.91 (d, *J* = 8.5 Hz, 2H), 7.47 (d, *J* = 8.1 Hz, 1H), 7.41 (s, 1H), 7.39 (d, *J* = 8.5 Hz, 2H), 6.96 (dd, *J* = 1.4, 8.1 Hz, 1H), 6.23 (brs, 2H), 5.68 (s, 2H), 5.63 (brs, 2H), 3.32–3.4 (m, 1H), 3.20 (s, 3H), 2.13 (q, *J* = 7.5 Hz, 2H), 1.67–2.03 (m, 8H), 0.97 (t, *J* = 7.5 Hz, 3H). HRMS (ESI) calcd for $\text{C}_{26}\text{H}_{31}\text{N}_6\text{O}_2\text{S}$ ($\text{M} + \text{H}$) $^+$ 491.2224, found 491.2230.

6-Ethyl-5-[1-(4-methanesulfonyl-benzyl)-2-phenyl-1H-benzimidazol-5-yl]-pyrimidine-2,4-diamine (compound 8b). ^1H NMR (300 MHz, $\text{DMSO}-d_6$) δ 7.88 (d, *J* = 8.1 Hz, 2H), 7.70–7.73 (m, 2H), 7.51–7.55 (m, 4H), 7.34 (d, *J* = 8.5 Hz, 2H), 7.04–7.06 (m, *J* = 9.8 Hz, 2H), 5.96 (brs, 2H), 5.72 (s, 2H), 5.58 (brs, 2H), 3.19 (s, 3H), 2.15 (q, *J* = 7.8 Hz, 2H), 0.99 (t, *J* = 7.8 Hz, 3H). HRMS (ESI) calcd for $\text{C}_{27}\text{H}_{27}\text{N}_6\text{O}_2\text{S}$ ($\text{M} + \text{H}$) $^+$ 499.1911, found 499.1921.

4-Benzyloxy-2-(4-nitrophenyl)-3-oxo-butyronitrile (9). To a solution of 4-nitrophenylacetone (10.0 g, 61.7 mmol), triethylamine (14.5 g, 144 mmol), and 4-(dimethylamino)pyridine (800 mg, 6.56 mmol) in CH_2Cl_2 (150 mL) at 0 $^\circ\text{C}$ was added benzyloxyacetyl chloride (12.0 g, 64.8 mmol) over 30 min. The resulting mixture was warmed to room temperature, stirred for 2 h, and concentrated in vacuo. The mixture was extracted in ethyl acetate (1 \times 150 mL) and washed with saturated NaHCO_3 (1 \times 80 mL), aqueous HCl (1 \times 80 mL), and brine (1 \times 80 mL). The organic layer was dried over MgSO_4 and concentrated in vacuo to provide crude 4-benzyloxy-2-(4-nitrophenyl)-3-oxo-butyronitrile **9** (19.6 g) as a red-brown solid which was used in the next step without further purification. ^1H NMR (300 MHz, $\text{DMSO}-d_6$) δ 8.24 (d, *J* = 9.2 Hz, 2H), 7.96 (d, *J* = 8.8 Hz, 2H), 7.25–7.46 (m, 5H), 4.60 (s, 2H), 4.48 (s, 2H); MS (APCI) *m/e* 311 ($\text{M} + \text{H}$) $^+$.

6-Benzyloxymethyl-5-(4-nitrophenyl)-pyrimidine-2,4-diamine (10). To a solution of compound **9** (9.72 g, 31.4 mmol) in CH_2Cl_2 (80 mL) was slowly added a solution of 2 M trimethylsilyldiazomethane (TMSCHN_2) in diethyl ether (30 mL, 60 mmol). The reaction was monitored by TLC using an aliquot to which had been added 3 M HOAc and was extracted in EtOAc. Glacial HOAc (5 mL) was added dropwise until the excess TMSCHN_2 was consumed as indicated by the absence of N_2 evolution. The mixture was concentrated in vacuo, extracted with EtOAc (1 \times 100 mL), and washed with 1 M HOAc (1 \times 150 mL) and brine (1 \times 100 mL). The organic layer was dried over MgSO_4 and concentrated in vacuo to provide 4-benzyloxy-3-methoxy-2-(4-nitrophenyl)-but-2-enitrile (10.2 g) which was used in the next step without further purification.

To a solution of 4-benzyloxy-3-methoxy-2-(4-nitrophenyl)-but-2-enitrile (10.2 g, 31.4 mmol) in EtOH (60 mL) was added a premixed solution of guanidine hydrochloride (3.605 g, 37.5 mmol) in EtOH (60 mL) and 2.65 M NaOEt in EtOH (14.2 mL, 37.6 mmol). The resulting dark, purple solution was heated at reflux for 3 h, concentrated in vacuo, extracted with EtOAc (1 \times 150

mL), and washed with 0.5 M NaOH (2 × 100 mL). The mixture was stirred vigorously, and then the resulting precipitate was filtered, providing 6-benzoyloxymethyl-5-(4-nitrophenyl)-pyrimidine-2,4-diamine **10** (8.78 g, 80% over 3 steps) as a light brown solid. ¹H NMR (300 MHz, DMSO-*d*₆) δ 8.19 (d, *J* = 8.8 Hz, 2H), 7.48 (d, *J* = 9.2 Hz, 2H), 7.18–7.31 (m, 3H), 7.05–7.17 (m, 2H), 6.13 (s, 2H), 5.90 (s, 2H), 4.30 (s, 2H), and 3.99 (s, 2H); MS (ESI) *m/e* = 352 (M + H)⁺.

5-(4-Amino-phenyl)-6-benzoyloxymethyl-pyrimidine-2,4-diamine (11). To a solution of 20 wt % Pd(OH)₂/C (wet, 600 mg) in MeOH (140 mL) was added 6-benzoyloxymethyl-5-(4-nitrophenyl)-pyrimidine-2,4-diamine **10** (5.00 g, 14.25 mmol) in a heavy walled high-pressure reaction vessel. The vessel was charged with H₂ (60 psi) and the mixture was stirred at room temperature for 14 h. The reaction mixture was filtered through a nylon membrane and the solution was concentrated in vacuo followed by trituration with MeOH (20 mL). 5-(4-Amino-phenyl)-6-benzoyloxymethyl-pyrimidine-2,4-diamine (**11**, 4.34 g, 95%) was obtained as a light yellow solid. ¹H NMR (300 MHz, DMSO-*d*₆) δ 7.16–7.37 (m, 5H) 6.85 (d, *J* = 8.1 Hz, 2H) 6.60 (d, *J* = 8.5 Hz, 2H) 5.86 (s, 2H) 5.49 (s, 2H) 5.12 (s, 2H) 4.35 (s, 2H) 3.97 (s, 2H); MS (ESI) *m/e* = 322 (M + H)⁺.

General Procedure for Synthesis of Amide Derivative: N-[4-(2,4-Diamino-6-benzoyloxymethyl-pyrimidin-5-yl)-phenyl]-acetamide (compound 13a). To a stirred solution of HOAc (9.3 mg, 0.16 mmol) and TBTU (70 mg, 0.22 mmol) in DMF (1 mL) were added 5-(4-amino-phenyl)-6-benzoyloxymethyl-pyrimidine-2,4-diamine **11** (50 mg, 0.16 mmol) and *N,N'*-diisopropylethylamine (0.27 mL, 1.56 mmol). After stirring at RT for 12 h, the product was precipitated by addition of H₂O (25 mL), dissolved in 2:1 MeOH/DMSO, and separated by preparative RP-HPLC to yield **13a** as an off-white solid (20 mg, 35%). ¹H NMR (300 MHz, DMSO-*d*₆) δ 9.99 (s, 1H), 7.61 (d, *J* = 8.5 Hz, 2H), 7.22–7.32 (m, 3H), 7.15–7.20 (m, 2H), 7.12 (d, *J* = 8.5 Hz, 2H), 6.03 (s, 2H), 5.68 (s, 2H), 4.33 (s, 2H), 3.96 (s, 2H), 2.06 (s, 3H). HRMS (ESI) calcd for C₂₀H₂₂N₅O₂ (M + H)⁺ 364.1768, found 364.1768. Anal. (C₂₀H₂₁N₅O₂ · 0.35 CF₃COOH) C, H, N.

The following compounds were prepared in a fashion similar to that for **13a** starting from common intermediate **11**.

N-[4-(2,4-Diamino-6-benzoyloxymethyl-pyrimidin-5-yl)-phenyl]-propionamide (compound 13b). ¹H NMR (300 MHz, DMSO-*d*₆) δ 9.91 (s, 1H), 7.63 (d, *J* = 8.5 Hz, 2H), 7.35–7.15 (m, 5H), 7.12 (d, *J* = 8.5 Hz, 2H), 5.99 (s, 2H), 5.64 (s, 2H), 4.33 (s, 2H), 3.96 (s, 2H), 2.34 (q, *J* = 7.6 Hz, 2H), 1.10 (d, *J* = 7.6 Hz, 3H). MS (ESI) 378 (M + H)⁺. Anal. (C₂₁H₂₃N₅O₂ · 0.4 CF₃COOH · 1.45 H₂O) C, H, N.

N-[4-(2,4-Diamino-6-benzoyloxymethyl-pyrimidin-5-yl)-phenyl]-3-methyl-butylamide (compound 13c). ¹H NMR (300 MHz, DMSO-*d*₆) δ 11.69 (s, 1H), 10.01 (s, 1H), 8.26 (s, 1H), 7.71 (d, *J* = 8.4 Hz, 2H), 7.26–7.35 (m, 5H), 7.14 (d, *J* = 8.7 Hz, 2H), 6.96 (s, 1H), 4.48 (s, 2H), 4.18 (s, 2H), 2.21 (d, *J* = 7.2 Hz, 2H), 2.05–2.14 (m, 1H), 0.95 (d, *J* = 6.9 Hz, 6H). HRMS (ESI) calcd for C₂₃H₂₈N₅O₂ (M + H)⁺ 406.2238, found 406.2236.

Cyclopropanecarboxylic Acid [4-(2,4-Diamino-6-benzoyloxymethyl-pyrimidin-5-yl)-phenyl]-amide (compound 13d). ¹H NMR (300 MHz, DMSO-*d*₆) δ 10.23 (s, 1H), 7.63 (d, *J* = 8.5 Hz, 2H), 7.15–7.33 (m, 5H), 7.12 (d, *J* = 8.5 Hz, 2H), 5.95 (brs, 2H), 5.60 (brs, 2H), 4.33 (s, 2H), 3.96 (s, 2H), 1.73–1.87 (m, 1H), 0.75–0.85 (m, 4H). HRMS (ESI) calcd for C₂₂H₂₄N₅O₂ (M + H)⁺ 390.1925, found 390.1925.

Cyclopentanecarboxylic Acid [4-(2,4-Diamino-6-benzoyloxymethyl-pyrimidin-5-yl)-phenyl]-amide (compound 13e). ¹H NMR (300 MHz, DMSO-*d*₆) δ 9.90 (s, 1H), 7.65 (d, *J* = 8.7 Hz, 2H), 7.15–7.32 (m, 5H), 7.12 (d, *J* = 8.7 Hz, 2H), 5.93 (brs, 2H), 5.59 (brs, 2H), 4.33 (s, 2H), 3.96 (s, 2H), 2.74–2.85 (m, 1H), 1.50–1.91 (m, 8H). HRMS (ESI) calcd for C₂₄H₂₈N₅O₂ (M + H)⁺ 418.2238, found 418.2242.

6-Benzoyloxymethyl-5-(4-methylamino-phenyl)-pyrimidine-2,4-diamine (compound 12). This intermediate was prepared by reductive amination of formaldehyde with **11**. 5-(4-amino-phenyl)-6-benzoyloxymethyl-pyrimidine-2, 4-diamine **11** (96 mg, 0.3 mmol)

was dissolved in MeOH (1 mL)/AcOH (50 μL). Formaldehyde 37% solution (27 μL, 0.36 mmol) was added and the mixture stirred for 15 min. NaBH₃CN (28 mg, 0.45 mmol) was then added, and the reaction mixture was stirred for 16 h at 25 °C. EtOAc (50 mL) was added, and the mixture was washed with saturated NaHCO₃ (20 mL) and brine (20 mL). The crude material was purified by reverse phase HPLC providing **12** as pale yellow solid (40 mg, 40%). ¹H NMR (300 MHz, DMSO-*d*₆) δ 7.33–7.18 (m, 5H), 6.93 (d, *J* = 8.5 Hz, 2H), 6.57 (d, *J* = 8.5 Hz, 2H), 5.88 (s, 2H), 5.71 (q, *J* = 5.1 Hz, 1H), 5.51 (brs, 2H), 4.35 (s, 2H), 3.97 (s, 2H), 2.70 (d, *J* = 5.1 Hz, 3H). MS (ESI) *m/e* 336 (M + H)⁺.

Cyclopentanecarboxylic Acid [4-(2,4-Diamino-6-benzoyloxymethyl-pyrimidin-5-yl)-phenyl]-methyl-amide (compound 13f). This compound was prepared in a fashion similar to that for **13a** substituting intermediate **12** for **11**. ¹H NMR (300 MHz, DMSO-*d*₆) δ 7.22–7.33 (m, 7H), 7.14–7.20 (m, 2H), 6.06 (brs, 2H), 5.80 (brs, 2H), 4.28 (s, 2H), 3.98 (s, 2H), 3.17 (s, 3H), 2.74–2.55 (m, 1H), 1.12–1.72 (m, 8H). HRMS (ESI) calcd for C₂₅H₃₀N₅O₂ (M + H)⁺ 432.2394, found 432.2397.

Tetrahydro-furan-2-carboxylic Acid [4-(2,4-Diamino-6-benzoyloxymethyl-pyrimidin-5-yl)-phenyl]-amide (compound 13g). ¹H NMR (300 MHz, DMSO-*d*₆) δ 9.73 (s, 1H), 7.55 (d, *J* = 8.5 Hz, 2H), 7.31–7.13 (m, 5H), 7.15 (d, *J* = 8.5 Hz, 2H), 6.01 (brs, 2H), 5.67 (brs, 2H), 4.43–4.36 (m, 1H), 4.33 (s, 2H), 4.03–3.96 (m, 1H), 3.96 (s, 2H), 3.88–3.81 (m, 1H), 2.24–2.15 (m, 1H), 2.05–1.83 (m, 3H). MS (APCI) *m/e* 420 (M + H)⁺. Anal. (C₂₃H₂₅N₅O₃ · 0.25 CH₃CN · 1.2 H₂O) C, H, N.

N-[4-(2,4-Diamino-6-benzoyloxymethyl-pyrimidin-5-yl)-phenyl]-isonicotinamide (compound 13h). ¹H NMR (500 MHz, DMSO-*d*₆) δ 10.65 (s, 1H), 8.85–8.76 (m, 2H), 7.94–7.80 (m, 4H), 7.36–7.23 (m, 7H), 4.49 (s, 2H), 4.20 (s, 2H). HRMS (ESI) calcd for C₂₄H₂₃N₆O₂ (M + H)⁺ 427.1877, found 427.1883.

N-[4-(2,4-Diamino-6-benzoyloxymethyl-pyrimidin-5-yl)-phenyl]-2-pyridin-3-yl-acetamide (compound 13i). ¹H NMR (300 MHz, DMSO-*d*₆) δ 10.30 (s, 1H), 8.55 (d, *J* = 1.7 Hz, 1H), 8.47 (dd, *J* = 4.7, 1.7 Hz, 1H), 7.72–7.80 (m, 1H), 7.63 (d, *J* = 8.5 Hz, 2H), 7.37 (dd, *J* = 7.5, 4.4 Hz, 1H), 7.09–7.31 (m, 7H), 5.95 (s, 2H), 5.60 (s, 2H), 4.32 (s, 2H), 3.95 (s, 2H), 3.72 (s, 2H). MS (ESI) *m/e* 441 (M + H)⁺. Anal. (C₂₅H₂₄N₆O₂ · 0.3 CF₃COOH · 0.75 H₂O) C, H, N.

N-(4-[2,4-Diamino-6-[(benzyloxy)methyl]pyrimidin-5-yl]phenyl)-thiophene-3-carboxamide (compound 13j). ¹H NMR (300 MHz, DMSO-*d*₆) δ 10.11 (s, 1H), 8.33–8.39 (m, 1H), 7.81 (d, *J* = 8.5 Hz, 2H), 7.69–7.62 (m, 2H), 7.15–7.33 (m, 7H), 5.97 (s, 2H), 5.64 (brs, 2H), 4.34 (s, 2H), 3.98 (s, 2H). MS (ESI) *m/e* 432 (M + H)⁺. Anal. (C₂₃H₂₁N₅O₂S · 0.9 H₂O) C, H, N.

N-(4-{2,4-Diamino-6-[(benzyloxy)methyl]pyrimidin-5-yl}-phenyl)-2-thien-3-ylacetamide (compound 13k). ¹H NMR (300 MHz, DMSO-*d*₆) δ 10.19 (s, 1H), 7.63 (d, *J* = 8.5 Hz, 2H), 7.49 (dd, *J* = 4.9, 2.9 Hz, 1H), 7.08–7.36 (m, 9H), 5.95 (s, 2H), 5.61 (brs, 2H), 4.32 (s, 2H), 3.95 (s, 2H), 3.67 (s, 2H). MS (ESI) *m/e* 441 (M + H)⁺. Anal. (C₂₄H₂₃N₅O₂ · 0.1 CF₃COOH) C, H, N.

2-(2-Bromothien-3-yl)-N-(4-{2,4-diamino-6-[(benzyloxy)methyl]pyrimidin-5-yl}phenyl)-acetamide (compound 13l). ¹H NMR (300 MHz, DMSO-*d*₆) δ 10.27 (s, 1H), 7.64 (d, *J* = 8.5 Hz, 2H), 7.58 (d, *J* = 5.8 Hz, 1H), 7.32–7.16 (m, 5H), 7.14 (d, *J* = 8.5 Hz, 2H), 7.06 (d, *J* = 5.4 Hz, 1H), 5.96 (s, 2H), 5.62 (s, 2H), 4.33 (s, 2H), 3.95 (s, 2H), 3.68 (s, 2H). HRMS (ESI) calcd for C₂₄H₂₂-BrN₅O₂S (M + H)⁺ 524.0750, found 524.0759.

N-(4-{2,4-Diamino-6-[(benzyloxy)methyl]pyrimidin-5-yl}-phenyl)-2-phenylacetamide (compound 13m). ¹H NMR (300 MHz, DMSO-*d*₆) δ 10.22 (s, 1H), 7.64 (d, *J* = 8.5 Hz, 2H), 7.09–7.40 (m, 12H), 5.95 (s, 2H), 5.60 (s, 2H), 4.32 (s, 2H), 3.94 (s, 2H), 3.65 (s, 2H). MS (ESI) *m/e* 440 (M + H)⁺. Anal. (C₂₆H₂₅N₅O₂ · 0.95 H₂O) C, H, N.

N-(4-{2,4-Diamino-6-[(benzyloxy)methyl]pyrimidin-5-yl}-phenyl)-3-phenylpropanamide (compound 13n). ¹H NMR (300 MHz, DMSO-*d*₆) δ 11.68 (s, 1H), 10.07 (s, 1H), 8.26 (s, 1H), 7.69 (d, *J* = 8.4 Hz, 2H), 7.17–7.37 (m, 10H), 7.14 (d, *J* = 8.4 Hz, 2H), 4.47 (s, 2H), 4.17 (s, 2H), 2.93 (t, *J* = 7.5 Hz, 2H), 2.67 (t,

$J = 7.6$ Hz, 2H). HRMS (ESI) calcd for $C_{27}H_{28}N_5O_2$ ($M + H$)⁺ 454.2238, found 454.2244.

General Procedure for Synthesis of Urea Derivative: 1-[4-(2,4-Diamino-6-benzyloxymethyl-pyrimidin-5-yl)-phenyl]-3-isopropyl-urea (compound 14a). To a solution of 5-(4-amino-phenyl)-6-benzyloxymethyl-pyrimidine-2, 4-diamine **11** (643 mg, 2.0 mmol) in THF (40 mL) was added *N,N'*-diisopropylethylamine (697 μ L, 4.0 mmol). A solution of triphosgene (198 mg, 0.67 mmol) in THF (2 mL) was then added, and a white precipitation was observed right away. The resulting mixture was stirred vigorously at room temperature for 10 min. Isopropylamine (852 μ L, 10.0 mmol) was added, the reaction mixture was stirred for another 10 min, and it was then partitioned between ethyl acetate (150 mL) and water (75 mL). The organic phase was washed with brine (50 mL), dried over $MgSO_4$, filtered, and concentrated in vacuo. The residue was purified by flash chromatography on silica gel column eluted with EtOH/MeOH (10:1) to provide compound **14a** as an off-white solid (618 mg, 77% yield). ¹H NMR (300 MHz, DMSO-*d*₆) δ 8.35 (s, 1H), 7.41 (d, $J = 8.8$ Hz, 2H), 7.32–7.16 (m, 5H), 7.06 (d, $J = 8.5$ Hz, 2H), 6.00 (d, $J = 7.8$ Hz, 1H), 5.93 (s, 2H), 5.58 (brs, 2H), 4.33 (s, 2H), 3.96 (s, 2H), 3.84–3.71 (m, 1H), 1.10 (d, $J = 6.5$ Hz, 3H). HRMS (ESI) calcd for $C_{22}H_{27}N_6O_2$ ($M + H$)⁺ 407.2190, found 407.2191. Anal. ($C_{22}H_{26}N_6O_2 \cdot 0.2 CF_3COOH$) C, H, N.

The following compounds were prepared according to a method similar to that of **14a**.

3-[4-(2,4-Diamino-6-benzyloxymethyl-pyrimidin-5-yl)-phenyl]-1-isopropyl-1-methyl-urea (compound 14b). ¹H NMR (300 MHz, DMSO-*d*₆) δ 8.26 (s, 1H), 7.54 (d, $J = 8.5$ Hz, 2H), 7.37–7.16 (m, 5H), 7.07 (d, $J = 8.5$ Hz, 2H), 5.97 (brs, 2H), 5.60 (brs, 2H), 4.40–4.55 (m, 1H), 4.34 (s, 2H), 3.97 (s, 2H), 2.80 (s, 3H), 1.09 (d, $J = 6.8$ Hz, 6H). HRMS (ESI) calcd for $C_{23}H_{29}N_6O_2$ ($M + H$)⁺ 421.2347, found 421.2350. Anal. ($C_{23}H_{28}N_6O_2 \cdot 0.35 CF_3COOH$) C, H, N.

***N*-(*tert*-Butyl)-*N'*-(4-{2,4-diamino-6-[(benzyloxy)methyl]pyrimidin-5-yl}phenyl)urea (compound 14c).** ¹H NMR (300 MHz, DMSO-*d*₆) δ 8.30 (s, 1H), 7.39 (d, $J = 8.5$ Hz, 2H), 7.35–7.16 (m, 5H), 7.05 (d, $J = 8.5$ Hz, 2H), 6.02 (s, 2H), 6.00 (s, 1H), 5.64 (brs, 2H), 4.35 (s, 2H), 3.98 (s, 2H), 1.30 (s, 9H). MS (ESI) *m/e* 421 ($M + H$)⁺. Anal. ($C_{23}H_{28}N_6O_2 \cdot 0.15 CF_3COOH$) C, H, N.

***N*-(4-{2,4-Diamino-6-[(benzyloxy)methyl]pyrimidin-5-yl}-phenyl)-*N'*-phenyl-urea (compound 14d).** ¹H NMR (300 MHz, DMSO-*d*₆) δ 8.80 (s, 1H), 8.74 (s, 1H), 7.54–7.43 (m, 4H), 7.34–7.23 (m, 5H), 7.17–7.22 (m, 2H), 7.12 (d, $J = 8.5$ Hz, 2H), 7.02–4.92 (m, 1H), 5.95 (s, 2H), 5.60 (s, 2H), 4.35 (s, 2H), 3.97 (s, 2H). HRMS (ESI) calcd for $C_{25}H_{25}N_6O_2$ ($M + H$)⁺ 441.2034, found 441.2038.

***N*-(Benzyloxy)-*N'*-(4-{2,4-diamino-6-[(benzyloxy)methyl]pyrimidin-5-yl}phenyl)urea (compound 14e).** ¹H NMR (500 MHz, DMSO-*d*₆) δ 7.50 (d, $J = 8.4$ Hz, 2H), 7.24–7.38 (m, 10H), 7.09 (d, $J = 8.4$ Hz, 2H), 4.48 (s, 2H), 4.32 (s, 2H), 4.19 (s, 2H). HRMS (ESI) calcd for $C_{26}H_{27}N_6O_2$ ($M + H$)⁺ 455.2190, found 455.2189.

***N*-(4-{2,4-Diamino-6-[(benzyloxy)methyl]pyrimidin-5-yl}-phenyl)-*N'*-(1-phenylethyl)urea (compound 14f).** ¹H NMR (300 MHz, DMSO-*d*₆) δ 8.45 (s, 1H), 7.42–7.16 (m, 12H), 7.05 (d, $J = 8.5$ Hz, 2H), 6.62 (d, $J = 7.8$ Hz, 1H), 5.93 (s, 2H), 5.58 (brs, 2H), 4.88–4.77 (m, 1H), 4.33 (s, 2H), 3.95 (s, 2H), 1.40 (d, $J = 7.1$ Hz, 3H). HRMS (ESI) calcd for $C_{27}H_{29}N_6O_2$ ($M + H$)⁺ 469.2347, found 469.2346. Anal. ($C_{27}H_{28}N_6O_2 \cdot 0.25 CF_3COOH$) C, H, N.

***N*-(4-{2,4-Diamino-6-[(benzyloxy)methyl]pyrimidin-5-yl}-phenyl)-*N'*-(2-phenylethyl)urea (compound 14g).** ¹H NMR (500 MHz, DMSO-*d*₆) δ 7.47 (d, $J = 8.5$ Hz, 2H), 7.21–7.36 (m, 11H), 7.08 (d, $J = 8.5$ Hz, 2H), 4.48 (s, 2H), 4.18 (s, 2H), 3.35 (t, $J = 7.0$ Hz, 2H), 2.77 (t, $J = 7.0$ Hz, 2H). HRMS (ESI) calcd for $C_{27}H_{29}N_6O_2$ ($M + H$)⁺ 469.2347, found 469.2350.

GHS-R Binding Assay. GHS-R binding assays were performed with membrane preparations. CHO-K cells expressing human ghrelin receptor (Euroscreen) were suspended in sucrose buffer (0.25–0.025% bacitracin) and disrupted by sonication using a vibra cell (Sonic and Materials Inc.) on 70% duty cycle in 15-s pulses on ice for 2.5 min. The homogenate was centrifuged at 60000g for

60 min, and pellets were suspended in Tris buffer (20 mM tris pH 7.4, 5 μ g/mL pepstatin-A, 0.1 mM PMSF and 3 mM EDTA). Binding reactions contained 1 μ g of membrane as determined by BCA protein assay (Pierce), 0.1 nM [¹²⁵I]-(-25 mM HEPES pH 7.4, 1 mM $CaCl_2$, 5 mM $MgSO_4$, and 0.5% protease free BSA). Incubations were carried out at room temperature for 2 h and were terminated by filtration using Filtermate Harvester (Perkin-Elmer) onto GF/C filter plates (Millipore) previously soaked in 0.5% polyethylenimine for 2 h. Filter plates were washed a minimum of 3 \times with cold wash buffer (binding buffer w/o BSA, supplemented with 0.5 M NaCl) to remove unbound counts, after which the filter plate bottoms were sealed and 50 μ L of MicroScint 20 was added to each well. Bound [¹²⁵I]-ghrelin was then determined by scintillation counting using Top Count NXT (Perkin-Elmer). The effects of compound were expressed as percent inhibition of [¹²⁵I]-ghrelin binding. Sigmoidal curves were fitted by Assay Explorer (MDL) software and IC₅₀ values determined.

GHS-R Ca²⁺ Flux Assay. CHO-K cells expressing human GHS-R (Euroscreen) were cultured in Ultra-CHO medium from BioWhittaker supplemented with 1% dialyzed FCS, 1% penicillin/streptomycin/fungizone, and 400 μ g/mL G418 (all from Life Technologies) at 37 °C in a humidified cell incubator containing 5% CO₂. Cells were plated in black 96-well plates with clear bottom (Costar) and cultured to confluency overnight. Prior to assay, cells were incubated in 100 μ L of Dulbecco's phosphate-buffered saline (DPBS) containing 1000 mg/L D-glucose, 36 mg/L sodium pyruvate, without phenol red (Life Technologies) with 1.14 mM Fluo-4 AM (Molecular Probes) and 0.25 M probenecid (Sigma) for 1–3 h in the dark at room temperature. The dye solution was aspirated, and the cells were washed twice with DPBS using the EL-450X cell washer (BioTech). After the last wash, 100 μ L of DPBS was added to each well. Cell plates were then transferred to the FLIPR unit (Molecular Probes). Compound additions were 50 μ L in duplicate or triplicate of 4 \times final concentration in DPBS containing 0.1% BSA and 4% DMSO. Fluorescence emissions from 96 wells were measured simultaneously at excitation and emission wavelength of 488 and 520 nm, respectively, for 3 min in 1-s intervals for the first minute and 5-s intervals thereafter. During this time agonist responses, if any, were recorded in the absence of ghrelin. Next, 50 μ L in duplicate or triplicate of 4 \times final concentration of ghrelin in DPBS containing 0.1% BSA and 4% DMSO were delivered within 1 s by an integrated 96-well pipettor. Fluorescence emissions were measured for another 3 min as above. During this time the antagonist effects of compounds on ghrelin-stimulated calcium flux were recorded. Sigmoidal curves were fitted and IC₅₀ and EC₅₀ values were determined by GraphPad Prism software. Ghrelin shows an EC₅₀ of 0.2 nM in this assay.

DHFR Assay. DHFR activity was determined by measuring the rate of depletion of NADPH, monitored at 340 nm, with a Beckman DU-7400 spectrophotometer that has a temperature controller set to 37 °C. Recombinant human DHFR (0.08 μ g/mL) (Sigma Chemicals, St. Louis, MO) and GHS-R antagonists, dissolved in DMSO, were mixed in a cuvette filled with a buffer containing 50 mM KH_2PO_4 , 0.25 M KCl, 10 mM β -mercaptoethanol, 100 μ M dihydrofolate, 100 μ M NADPH, pH 7.3. Total volume of the incubation was 800 μ L, and the amount of DMSO in the incubation was kept below 0.5%.

In Vivo Evaluation. All in vivo experiments were conducted in accordance with guidelines established by Abbott Laboratories' Animal Care and Use Committee and National Institutes of Health Guide for Care and Use of Laboratory Animals. In the first experiment, 200–250 g male Sprague–Dawley (CD) rats (Charles River Labs, Raleigh, NC) were individually housed 8 days prior to study and fed Teklad 8640 diet (Harlan-Teklad, Madison WI) ad libitum, with 12 h of light daily beginning at 06:00 h. Rats were acclimated to handling for 2 days prior to study. One day prior to study, body weight and food weight were measured, and rats were assigned to groups of equal mean body weight, with $n = 10$ per group. Body weights and food weight were again obtained on the day of study. Compounds or vehicle were administered by oral gavage, in 2 mL/kg volume, at approximately 09:00h (time 0).

Vehicle was 1% Tween-80 (Sigma Chemical Co., St. Louis, MO) in sterile water, pH adjusted to 3 with HCl. Compound formulations were also adjusted to pH 3 with HCl. Food was weighed at 2 h and 4 h after time 0. Eight hours after the first dose, food was weighed, and a second oral dose was administered. Food intake was determined at 12 h (4 h after second dose), 24, 32, and 48 h after the first dose.

Male C57BL/6J mice (age 5–6 weeks) were obtained from Jackson Labs (Bar Harbor, ME) for the second experiment, under conditions of 12 h lights on, 12 h lights off (on at 04:00 h), with food and water available ad libitum. Mice were fed a purified low fat diet (LF, D12450Bi, 10 kcal% fat, 3.8 kcal/g) or a high fat content diet (HF, D12492i, 60 kcal% fat, 5.2 kcal/g), both obtained from Research Diets Inc. (New Brunswick, NJ) for 16 weeks. Mice were housed in groups of 5 for the 13 weeks and then individually housed for the remainder of study. Mice were conditioned to oral gavage and daily vehicle administration for one week prior to drug administration. Mice were assigned to groups ($n = 12/\text{group}$) of equal mean body weight, and then treatments with compound formulations or vehicle were administered twice a day (BID) by oral gavage for two weeks. All compound doses are expressed as base equivalent weights per unit body weight. The vehicle used for conditioning and study was 1% Tween-80 in water. All doses were given in 4 mL vehicle per kg body weight, as base equivalent weights. Food weights and body weights were determined on days 0, 1, 4, 7, 11, and 14. On day 14, mice were humanely euthanized under CO₂ anesthesia. Terminal blood was obtained by cardiac puncture, placed in a tube containing EDTA anticoagulant, mixed by inversion, and maintained at 4 °C until centrifugation at 3000 rpm for 10 min. Plasma was stored at –80 °C until assay for leptin and insulin. Body composition (lean and fat mass) was determined after decapitation in a subgroup of 3 mice per treatment group by DEXA (PixiMus2, GE Lunar Corp, Madison WI), using software version 1.46. Epididymal fat pads were removed to obtain tissue weights. Plasma samples were assayed for leptin (Crystalchem, Downers Grove, IL) and insulin (Alpco Diagnostics, Windham NH) by ELISA. The sensitivities, intra-assay and inter-assay coefficients of variation for these assays are as follows: leptin 0.2 ng/mL, 5.4% and 6.9%; and insulin 0.07 ng/mL, 3.3%, 1.8%.

The third study examined acute feeding in male diet-induced obese mice after 16 weeks on high fat diet as indicated in the second experiment. Mice were housed individually for 4 weeks prior to study, acclimated to handling, and assigned to treatment groups of equal mean body wt ($n = 10/\text{group}$) the day before study and then fasted for 24 h. At approximately 09:00 h, mice were administered vehicle (sterile nonpyrogenic, 0.9% sodium chloride, adjusted to pH 3 with HCl) or compound by intraperitoneal injection, in 4 mL/kg. One hour after injection, measured food bins were placed in the cages. Food intake was determined at 20 min, 1, 2, 4, and 24 h after time 0 refeeding time. Cumulative food intake vs time (20 min, 1, 2, 4, and 24 h) for each treatment was calculated as percent of mean vehicle group food intake.

Statistical analyses of body weight change and food intake data over time, terminal plasma analytes, DEXA, and tissue weight data were performed by one-way analysis of variance, and if significant, followed by Dunnett's test, using GraphPad InStat (Graphpad, San Diego, CA). Differences were considered significant where $p < 0.05$. Data are presented as mean \pm SEM.

Acknowledgment. The authors are grateful to Dr. Ying Wang and Anita K. McGreal for their assistance in high-throughput syntheses and purification. Thanks are also due to Dr. Paul Richardson for synthesis of peptide antagonist [D-Lys-3]-GHRP-6.

Supporting Information Available: Elemental analysis data for compounds **13a–14f**. This material is available free of charge via the Internet at <http://pubs.acs.org>.

References

- (1) Smith, R. G.; Jiang, H.; Sun, Y. Developments in Ghrelin Biology and Potential Clinical Relevance. *Trends Endocrinol. Metab.* **2005**, *16*, 436–42.
- (2) a) Kojima, M.; Hosoda, H.; Date, Y.; Nakazato, M.; Matsuo, H.; Kangawa, K. Ghrelin is a Growth-Hormone-Releasing Acylated Peptide From Stomach. *Nature* **1999**, *402*, 656–660. (b) Kojima, M.; Hosoda, H.; Matsuo, H.; Kangawa, K. Ghrelin: Discovery of the Natural Endogenous Ligand for the Growth Hormone Secretagogue Receptor. *Trends Endocrinol. Metab.* **2001**, *12*, 118–122.
- (3) Korbonits, M and Grossman, AB. Ghrelin: update on a novel hormonal system. *Eur. J. Endocrinol.* **2004**, *151 Suppl 2*: S67–S70.
- (4) Kojima, M.; Kangawa, K. Ghrelin: structure and function. *Physiol. Rev.* **2000**, *85*, 495–522.
- (5) van der Lely, A. J.; Tschopp, M.; Heiman, M. L.; Ghigo, E. Biological, physiological, pathophysiological, and pharmacological aspects of ghrelin. *Endocr. Rev.* **2004**, *25* (3), 426–457.
- (6) Tschopp, M.; Smiley, D. L.; Heiman, M. L. Ghrelin induces adiposity in rodents. *Nature* **2000**, *407*, 908–913.
- (7) Cummings, D. E.; Purnell, J. Q.; Frayo, R. S.; Schmidova, K.; Wisse, B. E.; Weigle, D. S. A preprandial rise in plasma ghrelin levels suggests a role in meal initiation in human. *Diabetes* **2001**, *50*, 1714–1719.
- (8) Nakazato, M.; Murakami, N.; Date, Y.; Kojima, M.; Matsuo, H.; Kangawa, K.; Matsukura, S. A role for ghrelin in the central regulation of feeding. *Nature* **2001**, *409*, 194–198.
- (9) Asakawa, A.; Inui, A.; Kaga, T.; Katsurura, G.; Fujimiya, M.; Fujino, M. A.; Kasuga, M. Antagonism of ghrelin receptor reduces food intake and body weight gain in mice. *Gut* **2003**, *52*, 947–952.
- (10) Shearman, L. P.; Wang, S. P.; Helmling, S.; Stribling, D. S.; Mazur, P.; Ge, L.; Wang, L.; Klussmann, S.; Macintyre, D. E.; Howard, A. D.; Strack, A. M. Ghrelin Neutralization by a Ribonucleic Acid-SPM Ameliorates Obesity in Diet-Induced Obese Mice. *Endocrinology* **2006**, *147*, 1517–1526.
- (11) Cheng, K.; Chan, W. W. S.; Butler, B.; Wei, L.; Smith, R. G. A novel non-peptidyl growth hormone secretagogue. *Horm. Res.* **1993**, *40*, 109–115.
- (12) Zhao, H.; Liu, G. Growth hormone secretagogue receptor antagonists as anti-obesity therapies: still an open question. *Current Opin. Drug. Discovery Dev.* **2006**, in press.
- (13) Liu, B.; Liu, G.; Xin, Z.; Serby, M.; Zhao, H.; Schaefer, V.; Falls, D.; Kaszubska, W.; Collins, C.; Sham, H. Novel isoxazole carboxamides as growth hormone secretagogue receptor (GHS-R) antagonists. *Bioorg. Med. Chem. Lett.* **2004**, *14*, 5223–5226.
- (14) Xin, Z.; Zhao, H.; Serby, M.; Liu, B.; Schaefer, V.; Falls, D.; Kaszubska, W.; Collins, C.; Sham, H.; Liu, G. Synthesis and structure–activity relationships of isoxazole carboxamides as growth hormone secretagogue receptor antagonists. *Bioorg. Med. Chem. Lett.* **2005**, *15*, 1201–1204.
- (15) Zhao, H.; Xin, Z.; Liu, G. Schaefer, V.; Falls, D.; Kaszubska, W.; Collins, C.; Sham, H. Discovery of tetralin carboxamide growth hormone secretagogue receptor antagonists via scaffold manipulation. *J. Med. Chem.* **2004**, *47*, 6655–6657.
- (16) Zhao, H.; Xin, Z.; Patel, J. R.; Nelson, L. T. J.; Liu, B.; Szczepankiewicz, B. G.; Schaefer, V.; Falls, D.; Kaszubska, W.; Collins, C.; Sham, H.; Liu, G. Structure–activity relationship studies on tetralin carboxamide growth hormone secretagogue receptor antagonists. *Bioorg. Med. Chem. Lett.* **2005**, *15*, 1825–1828.
- (17) Serby, M.; Zhao, H.; Szczepankiewicz, B.; Kosogof, C.; Xin, Z.; Liu, B.; Liu, M.; Nelson, L.; Kaszubska, W.; Falls, D.; Schaefer, V.; Bush, E.; Shapiro, R.; Droz, B.; Knourek-Segel, V.; Fey, T.; Brune, M.; Beno, D.; Turner, T.; Collins, C.; Jacobson, P.; Sham, H.; Liu, G. 2,4-Diaminopyrimidine derivatives as potent growth hormone secretagogue receptor antagonists. *J. Med. Chem.* **2006**, *49*, 2568–2578.
- (18) Sirotnak, F. M.; Burchall, J. J.; Ensminger, W. B.; Montgomery, J. A., Eds. *Folate Antagonists as Therapeutic Agents*; Academic Press: New York, 1984.
- (19) Weir, E. C.; Cashmore, A. R.; Dreyer, R. N.; Graham, M. L.; Hsiao, N.; Moroson, B. A.; Sawicki, W. L.; Bertino, J. R. Pharmacology and toxicity of a potent “nonclassical” 2,4-diamino quinazoline folate antagonist, trimetrexate, in normal dogs. *Cancer Res.* **1982**, *42*, 1696–1702.
- (20) Griffin, R. J.; Schwalbe, C. H.; Stevens, M. F. G.; Wong, K. P. Structure studies on bio-active compounds. Part 3. Reexamination of the hydrolysis of the antimalarial drug pyrimethamine and related derivatives and crystal structure of a hydrolysis product. *J. Chem. Soc., Perkin Trans. 1* **1985**, 2267–2276

- (21) Robson, C.; Meek, M.; Grunwaldt, J.; Lambert, P.; Queener, S.; Schmidt, D.; Griffin, R. Nonclassical 2,4-diamino-5-aryl-6-ethylpyrimidine antifolates: activity as inhibitors of dihydrofolate reductase from pneumocystis carinii and toxoplasma gondii and as antitumor agents. *J. Med. Chem.* **1997**, *40*, 3040–3048.
- (22) Rotella, D. P.; Sun, Z.; Zhu, Y.; Krupinski, J.; Pongrac, R.; Seliger, L.; Normandin, D.; Macor, J. E. N-3-Substituted imidazoquinazolines: potent and selective PDE5 inhibitors as potential agents for treatment of erectile dysfunction. *J. Med. Chem.* **2000**, *43*, 1257–1263.
- (23) Nocolai, E.; Goyard, J.; Benchetrit, T.; Teulon, J.; Caussade, F.; Virone, A.; Delchambre, C.; Cloarec, A. Synthesis and structure–activity relationships of novel benzimidazole and imidazo[4,5-b]pyridine acid derivatives as thromboxane A2 receptor antagonists. *J. Med. Chem.* **1993**, *36*, 1175–1187.
- (24) Smith, K.; El-Hiti, G.; Hawes, A. Carbonylation of doubly lithiated *N'*-aryl-*N*, *N*-dimethylureas: A novel approach to isatins via intramolecular trapping of acyllithiums. *Synthesis* **1993**, *36*, 1175–1187.
- (25) Liu, B.; Liu, M.; Xin, Z.; Zhao, H.; Serby, M.; Kosogof, C.; Nelson, L.; Szczepankiewicz, B.; Kaszubska, W.; Schaefer, V.; Falls, D.; Lin, C.; Collins, C.; Sham, H.; Liu, G. Optimization of 2,4-diaminopyrimidines as GHS-R antagonists: side chain exploration. *Bioorg. Med. Chem. Lett.* **2006**, *16*, 1864–1868.
- (26) Griffin, R. J.; Meek, M. A.; Schwalbe, C. H.; Stevens, M. F. G. Structural studies on bioactive compounds. Part 8. Synthesis, crystal structure, and biological properties of a new series of 2,4-diamino-5-aryl-6-ethylpyrimidine dihydrofolate reductase inhibitors with in vivo activity against a methotrexate-resistant cell line. *J. Med. Chem.* **1989**, *32*, 2468–2474.
- (27) Hutchins, C. W. Three-dimensional models of the D1 and D2 dopamine receptors. *Endocr. J.* **1994**, *2*, 7–23.
- (28) Hutchins, C. W. Structure and Function of 7TM Receptors. Schwartz, T., W.; Hjorth, S., A.; Kastrup, J., S., Eds. *Alfred Benzon Symposium 39*; Munksgaard: Copenhagen, 1996; pp 213–226.
- (29) Geneste, H.; Backfisch, G.; Braje, W.; Delzer, J.; Haupt, A.; Hutchins, C., W.; King, L., L.; Kling, A.; Teschendorf, H.-J.; Unger, L.; Wernet, W. Synthesis and SAR of highly potent and selective dopamine D(3)-receptor antagonists: 1H-pyrimidin-2-one derivatives. *Bioorg. Med. Chem. Lett.* **2006**, *16*, 490–494.
- (30) Cummings, D. E.; Foster-Schubert, K. E.; Overduin, J. Ghrelin and energy balance: Focus on current controversies. *Curr. Drug Targets* **2005**, *6*, 153–169.
- (31) Date, Y.; Murakami, N.; Toshinai, K.; Matsukura, S.; Nijijima, A.; Matsuo, H.; Kangawa, K.; Nakazato, M. The role of the gastric afferent vagal nerve in ghrelin-induced feeding and growth hormone secretion in rats. *Gastroenterology* **2002**, *123*, 1120–1128.
- (32) Asakawa A, Inui A, Kaga T, Yuzuriha H, Nagata T, Ueno N, Makino S, Fujimiya M, Nijijima A, Fujino MA, Kasuga M. Ghrelin is an appetite-stimulatory signal from stomach with structural resemblance to motilin. *Gastroenterology* **2001**, *120*, 337–345.
- (33) le Roux, C. W.; Neary, N. M.; Halsey, T. J.; Small, C. J.; Martinez-Isla, A. M.; Ghatei, M. A.; Theodorou, N. A.; Bloom, S. R. Ghrelin does not stimulate food intake in patients with surgical procedures involving vagotomy. *J. Clin. Endocrinol. Metab.* **2005**, *90*, 4521–4524.

JM060461G